

*Supporting Information*

**Flexible and multifunctional electronics fabricated by a solvent-free and user-friendly method**

By *Toan Dinh*,<sup>\*a</sup> *Hoang-Phuong Phan*,<sup>a</sup> *Afzaal Qamar*,<sup>a</sup> *Nam-Trung Nguyen*,<sup>a</sup> and *Dzung Viet Dao*<sup>a,b</sup>

<sup>a</sup> Queensland Micro- and Nanotechnology Centre, Griffith University, Queensland, Australia.

<sup>b</sup> School of Engineering, Griffith University, Queensland, Australia.

\* Email of corresponding author: *toan.dinh@griffithuni.edu.au*

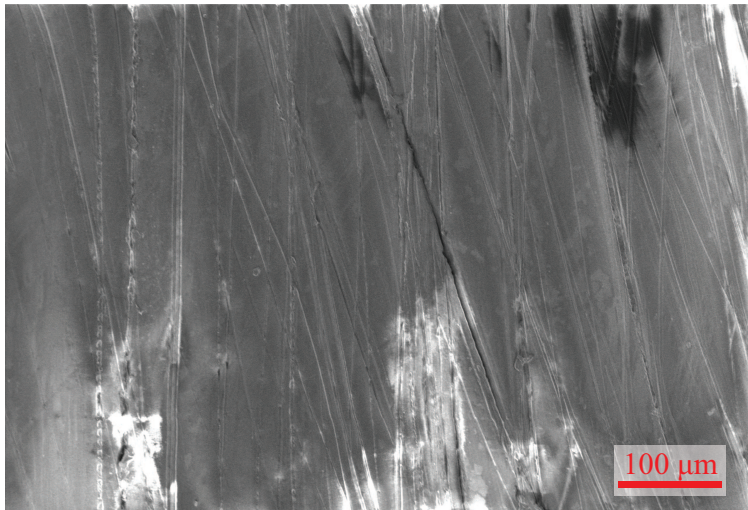


Figure 1: Scanning Electron Microscope (SEM) image of the PVC surface.

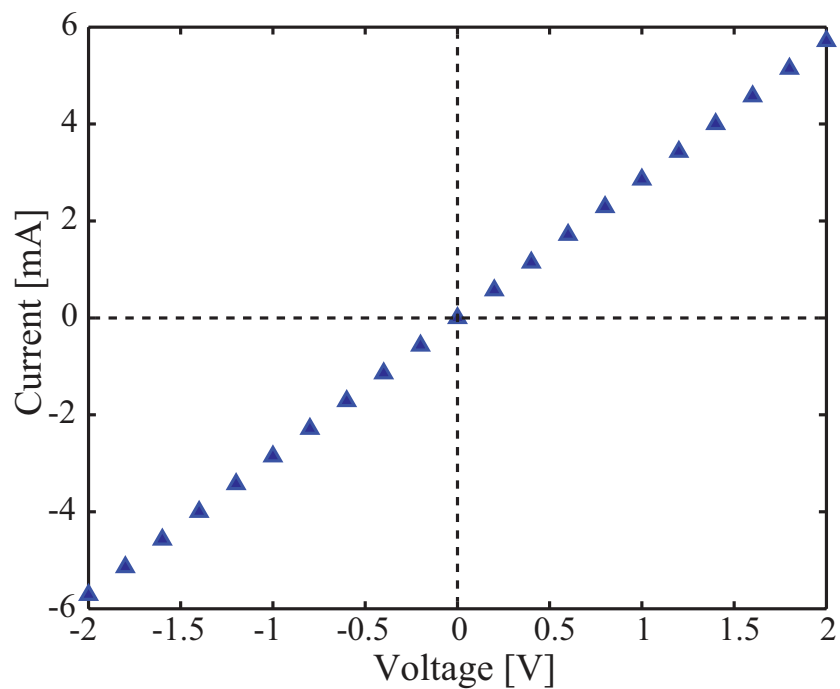


Figure 2: Current-voltage characteristics of the graphite film deposited on a PVC substrate. The linear relationship between the applied voltage and measured current indicates a good Ohmic contact behaviour of the graphite film and its electrode (silver epoxy). This result also shows that the graphite film on PVC can be used as a suitable resistive element for thermal effects.

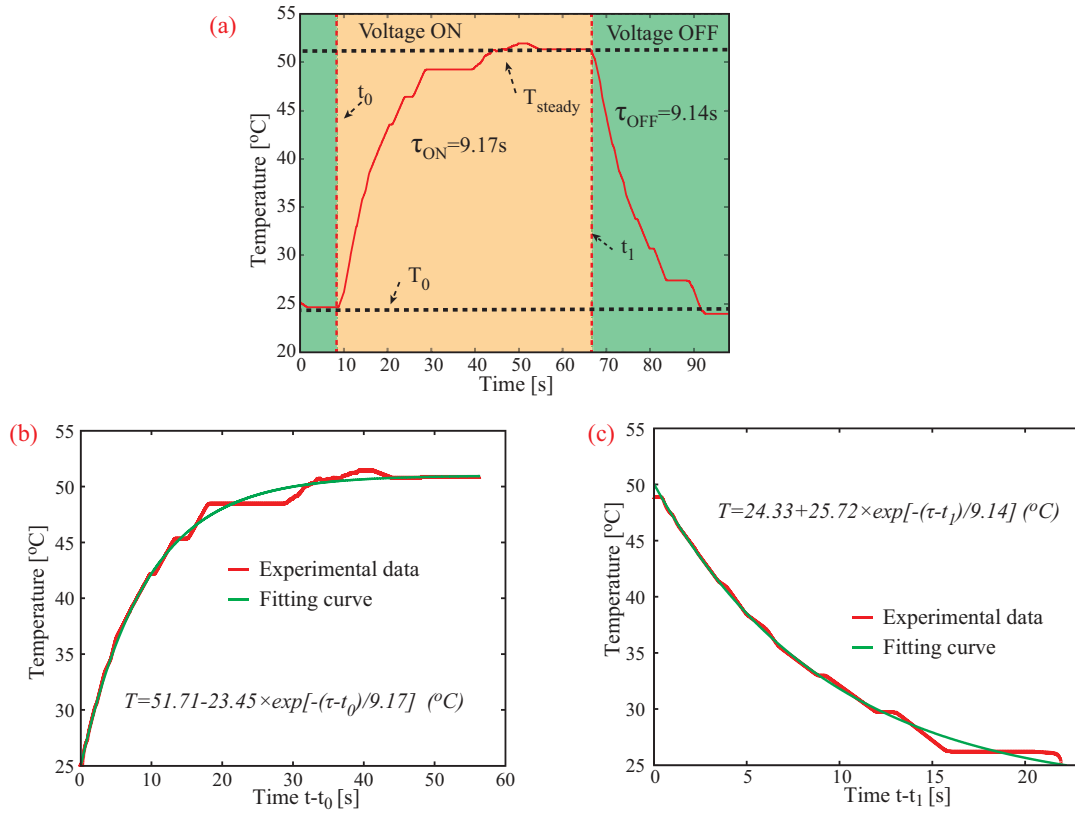


Figure 3: Time response of the heater. (a) Temperature profile of the heater under a cycle with initial temperature  $T_0$ , steady-state temperature  $T_{steady}$ , time  $t_0$ ,  $t_1$  at that voltage is ON, OFF, respectively. (b) Exponential fit for time response of 9.17 s for temperature rising. (c) Exponential fit for time response of 9.14 s for temperature decreasing. The time responses obtained from fitting curves of the measured temperature. For both heating and cooling processes, the time responses show a consistent value of approximately 9 s.

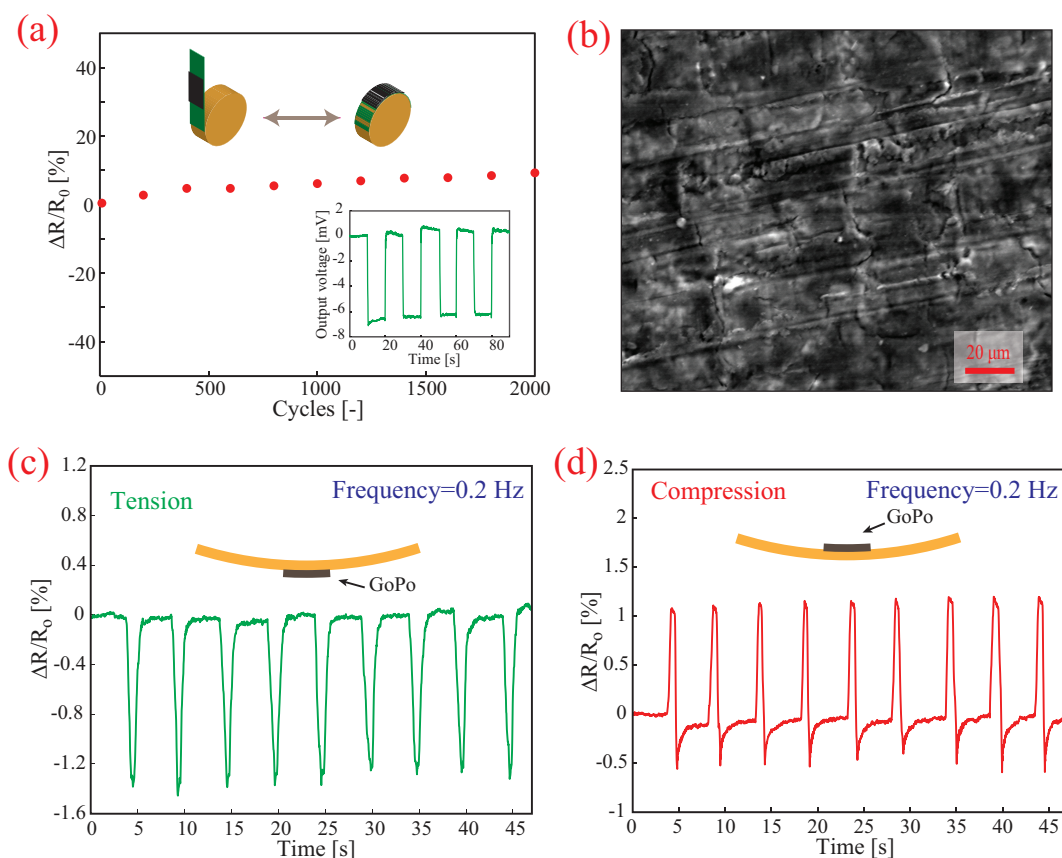


Figure 4: a) The relative resistance change under both tension of 0.28% strain for 2000 cycles. The inset shows the good repeatable response of the strain gauge under 0.28% strain. b) Scanning Electron Microscope (SEM) image of the graphite film after 2000 cycles of bending. The microcracks occur resulting on an increase in the electrical resistance. c,d) Performance of the GoPo strain gauge under c) tension and d) compression.

The reliability of the strain element was evaluated by subjecting the strain gauge to various bending cycles in which the strain element was repeatedly subjected to a 0.28% strain and then released. It is worth noting that the electrical resistance of pencil graphite drawn on PVC increased with increasing cycles of test, and the relative resistance change was up to approximately 10% after 2000 cycles (as shown in Figure 4a). There are two possible reasons for this large electrical resistance change. Firstly, it is well known that the graphite could be come off under stress/strain which could result in a decrease of the number of electrical contacts/chains in the graphite particle network (see Figure 4a in the main manuscript). Therefore, the electrical paths for carriers to transport decrease, which lead to an increase of the electrical resistance. Secondly, the resistance change with lifetime tests can also be attributed to the fact that there was an increase in the number of microcracks in the graphite film with an increasing number of testing cycles (4b). In addition, the obtained results agree with the resistance change of more than 10% for 10000 cycles of graphite drawn on paper at a strain of 0.32% reported in Reference [29] (main manuscript). After the life-time test, we confirmed the stable performance of the strain element under 0.28% strain, as shown in the inset Figure 4b. The obtained stable and repeatable response indicates the reliability of GoPo. Furthermore, we evaluated the dynamic

response of a GoPo strain sensor to monitor the tensile and compressive behaviour of a flexible structure surface where tensile and compressive stresses were applied for various cycles. Figures 4c and d illustrate the excellent dynamic response of the 0.2 Hz signals for both tension and compression which reveals the potential of using GoPo for structural real-time observing systems. In addition, the high signal-to-noise ratio was observed, indicating that the strain gauge offered a high strain resolution which was valuable for detecting small strain signals.

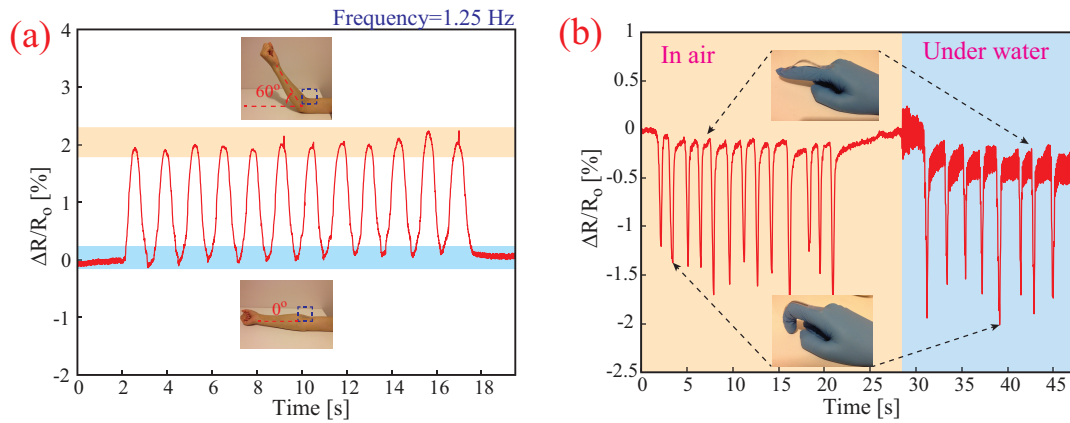


Figure 5: Wearable GoPo strain sensors for human motion detection. a) Dynamic bending behaviour of human arm monitored by a GoPo strain sensor at a frequency of 1.25 Hz and a bending angle of 60°. The lower inset and the upper inset show the initial and 60° positions, respectively. b) Response of the sensor in finger bending test in air and under water.

Figure 5a shows a real-time response of the sensor at two angles of 0° and 60°, which indicates its rapid response and repeatability. At the initial position, the bending angle is zero degrees (lower inset Figure 5a), and no strain is applied, the relative resistance change is zero (lower peak points, Figure 5a). The signals reach the higher peak points when the arm is at 60°.

We also demonstrated the use of a GoPo strain gauge covered by an insulation epoxy layer for human-motion detection in different environments (e.g. in air and under water), as shown in Figure 5b. The performance of the sensor was continuously observed when the sensor was affixed to a human finger and moved from air to water. Larger noise signals were suddenly observed when the sensor reached the air-water interface, which reduced the signal-to-noise ratio and thus the strain resolution for human detection was lower under water than in air. This noise was attributed to the complex dynamic movement of water induced by the finger movement. The sensor responded repeatedly and rapidly with the motion of the finger, indicating that the GoP sensor was suitable for wearable devices since it was able to measure different parts of the human body.

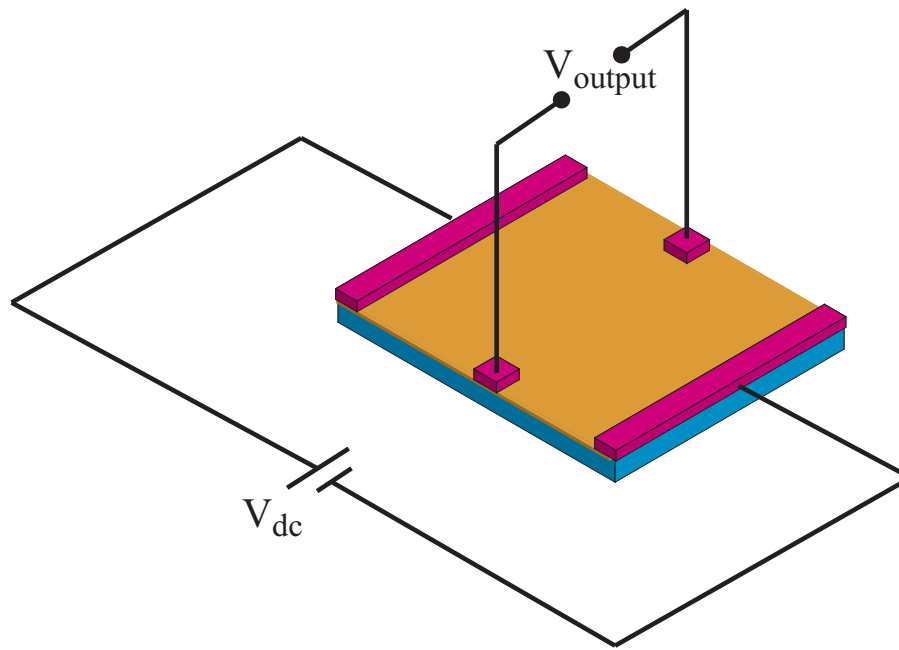


Figure 6: Four-point measurement setup for human motion detection. A voltage of 10 V was applied while the output voltage ( $V_{output}$ ) was measured real-time to perceive the human wrist motion.



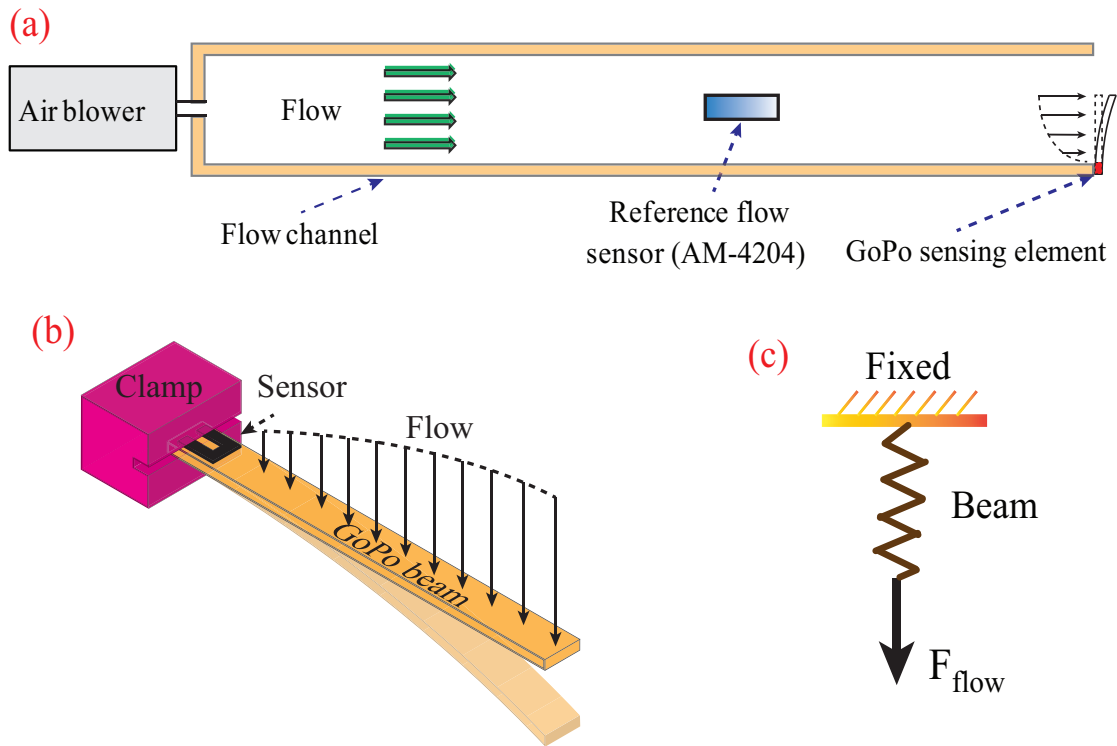


Figure 7: Flow measurement details. (a) Flow measurement setup for the drag force flow measurement. (b) Deformation of the GoPo sensing beam under flows. (c) Mechanical model for the elastic beam. The flow drag force was generated and deformed the beam, leading to the stress/strain at the GoPo sensing element. By measuring the resistance change of the GoPo element, the air velocity is defined.